

On the use of the Reynolds decomposition in the intermittent region of turbulent boundary layers

Y. S. Kwon^{1,†}, N. Hutchins¹ and J. P. Monty¹

¹Department of Mechanical Engineering, University of Melbourne, Victoria 3010, Australia

(Received 8 July 2015; revised 11 September 2015; accepted 23 February 2016;
first published online 30 March 2016)

In the analysis of velocity fields in turbulent boundary layers, the traditional Reynolds decomposition is universally employed to calculate the fluctuating component of streamwise velocity. Here, we demonstrate the perils of such a determination of the fluctuating velocity in the context of structural analysis of turbulence when applied in the outer region where the flow is intermittently turbulent at a given wall distance. A new decomposition is postulated that ensures non-turbulent regions in the flow do not contaminate the fluctuating velocity components in the turbulent regions. Through this new decomposition, some of the typical statistics concerning the scale and structure of turbulent boundary layers are revisited.

Key words: turbulent boundary layers, turbulent flows

1. Introduction

In 1895, Reynolds presented his paper showing a velocity decomposition based on the temporal mean of the velocity (Reynolds 1895). Ever since, this decomposition has been employed in many fluid flow scenarios and almost universally in wall turbulence. In contrast, in a variety of other turbulent or chaotic flows (particularly in periodic flows), a triple decomposition is used (e.g. Hussain & Reynolds 1970; Lyn & Rodi 1994) to isolate organised systematic variations in velocity which do not contribute to the local structure of the chaotic or turbulent flow.

In the analysis of the structure of turbulence, regions with spatially coherent velocity fluctuations are often interpreted as a signifier of organised turbulent motions. Hence, conclusions on the structure of turbulent boundary layers (TBLs) have often been drawn from the instantaneous observation and statistical analysis of the fluctuating velocity components under the Reynolds decomposition (e.g. Tomkins & Adrian 2003; Hutchins & Marusic 2007; Sillero, Jiménez & Moser 2014). However, when extending these analyses into the outer region of a TBL, where the flow is intermittently turbulent, the appropriateness of applying the Reynolds decomposition needs to be questioned. In the intermittent region, two different states (turbulent and non-turbulent), each of which have different means, can exist at different times. Under the Reynolds decomposition, both of these states are reduced to a single common mean. This decomposition is problematic for a number of reasons, and counter-intuitively gives rise to turbulent fluctuations in the non-turbulent region.

† Email address for correspondence: kwon@unimelb.edu.au

In fact, the adequacy of representing turbulent and non-turbulent regions, each having different mean velocities, by a single common mean velocity has been questioned for more than 70 years (Corrsin 1943). However, practical difficulties with extracting the measurement signal residing inside the turbulent or non-turbulent region delayed the application of this idea to rigorous quantitative analysis until the 1970s. With the development of conditional sampling of hot-wire anemometry, Kovaszny, Kibens & Blackwelder (1970) represented turbulent and non-turbulent zones of the TBL with separate ‘zonal’ mean velocities for each respective region. Further examples of boundary layer studies that have attempted to represent turbulent and non-turbulent regions by different mean velocities of each region include Antonia (1972) and Hedley & Keffer (1974). Around the same time, a similar approach was also applied to free-shear flows such as mixing layers (e.g. Wygnanski & Fiedler 1970), jets (e.g. Antonia, Prabhu & Stephenson 1975; Gutmark & Wygnanski 1976) and wakes (e.g. Fabris 1979). Having observed that the turbulent and non-turbulent regions have different zonal mean velocities, those studies defined the fluctuating velocity components with respect to the zonal mean velocities for each respective region as opposed to the Reynolds-averaged mean velocities across two different regions. This allowed the examination of the statistical behaviour of each flow region independently without the influence from the other, which cannot be isolated under the Reynolds decomposition. However, owing to the limitation of hot-wire anemometry as a single-point measurement, these investigations were mainly restricted to single-point statistics of the flow in each zone (e.g. turbulent intensity, turbulent shear stress, higher-order velocity moments, energy budget terms).

In this paper, issues with applying the Reynolds decomposition in the intermittent region of a TBL in the analysis of the structure of turbulence are demonstrated and a new way of decomposing the total velocity is proposed where the turbulent flow and non-turbulent free stream are treated separately. Then, some of the typical statistics related to the scale and structure of turbulence are computed through this new decomposition and compared with those from the traditional Reynolds velocity fluctuations.

2. Dataset

In this paper, the streamwise–wall-normal planes extracted from direct numerical simulation (DNS) of a TBL (Sillero, Jiménez & Moser 2013) are examined. The friction Reynolds number $Re_\tau = \delta U_\tau / \nu$ at the middle of the streamwise domain of extracted fields is 1780, where δ , U_τ and ν denote the boundary layer thickness, friction velocity and kinematic viscosity, respectively. The boundary layer thickness is determined by fitting the composite velocity profile of Chauhan, Monkewitz & Nagib (2009) at the middle of the streamwise domain of extracted fields and it is approximately 25% greater than the 99% boundary layer thickness. The streamwise domain of extracted fields is 9δ and it is chosen to be sufficiently long to observe the large-scale features in the flow while minimising the Reynolds-number variation within the streamwise domain. Across this streamwise domain, Re_τ based on the local boundary layer thickness varies from 1659 to 1888, corresponding to $Re_\theta = \theta U_\infty / \nu = 4000$ to 4630, where θ is the momentum thickness and U_∞ is the free-stream velocity. The flow field is considered to have recovered from the inflow conditions at those Reynolds numbers (Sillero *et al.* 2013).

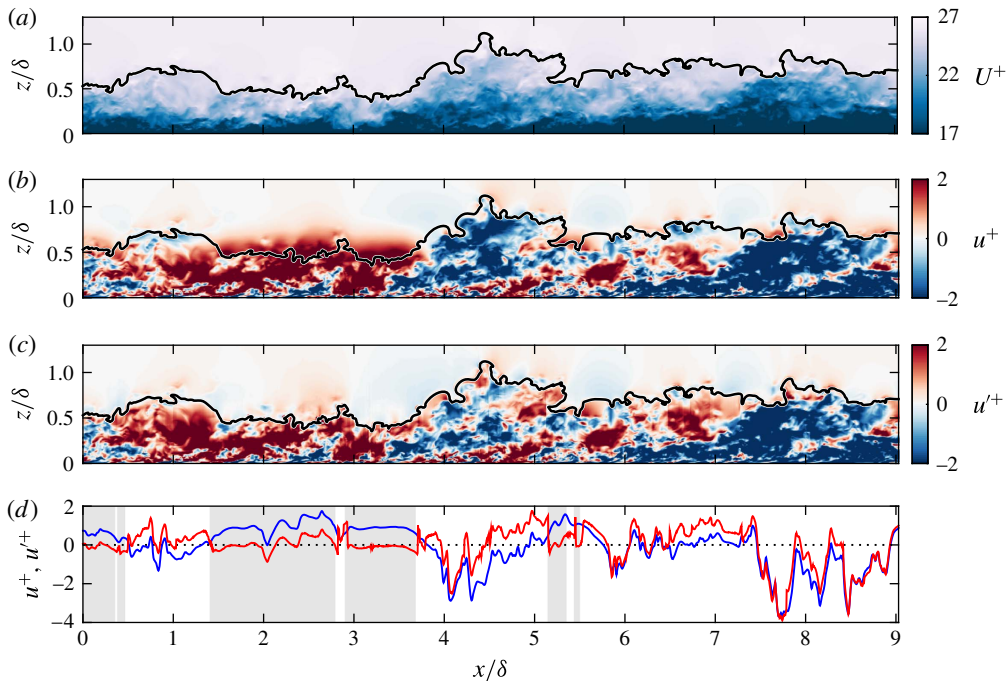


FIGURE 1. (a) Instantaneous streamwise velocity field; (b) fluctuating velocity field using the traditional Reynolds decomposition; and (c) fluctuating velocity field determined using the new decomposition method. Black lines show the turbulent/non-turbulent interface. (d) The streamwise velocity fluctuations as a function of the streamwise position at $z = 0.6\delta$. Blue and red lines represent the fluctuations under the Reynolds decomposition, u , and the new decomposition, u' , respectively. Horizontal dotted line indicates the zero level, and the grey shadings are in the free stream.

3. A new decomposition

Figure 1 shows an instantaneous streamwise velocity field of a TBL. Throughout this paper, x and z denote the streamwise and wall-normal coordinates, respectively, and U and W denote the total instantaneous velocity components in the corresponding directions. Velocity quantities with an overline indicate the temporal mean, and the fluctuating velocity components about the temporal mean are represented by lower-case variables (e.g. $U = \bar{U} + u$; Reynolds decomposition). The superscript ‘+’ represents normalisation by inner scales (ν/U_τ for length and U_τ for velocity). The heavy black lines in figure 1(a–c) represent the turbulent/non-turbulent interface (TNTI), which is determined using the kinetic energy criteria of Chauhan *et al.* (2014).

In the fluctuating streamwise velocity field based on the Reynolds decomposition (figure 1b), one can observe that the region of strongly positive Reynolds fluctuation actually extends across the TNTI into the free stream when the TNTI height is low (at $x/\delta \simeq 2$ –3 in figure 1b). This is mathematically correct because the free stream is a region with positive velocity fluctuation relative to the temporal mean streamwise velocity at this wall-normal location. However, one should not consider it as a region of ‘turbulent’ fluctuation since it exists in the non-turbulent free stream as a consequence of the oscillation of the TNTI and does not really signify the presence

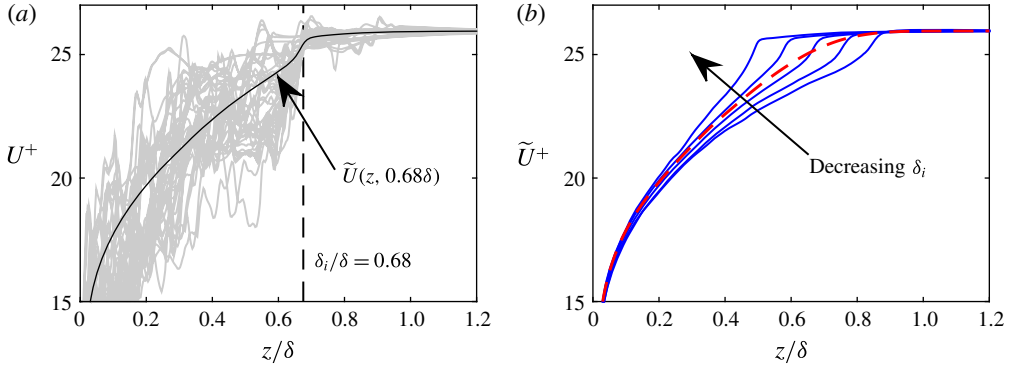


FIGURE 2. (Colour online) (a) Grey lines are randomly selected instantaneous total velocity profiles at x locations where the TNTI is at 68% of the boundary layer thickness. Solid line is the ensemble average of all such instantaneous velocity profiles. (b) Conditional mean velocity profiles (blue solid lines) for a range of interface heights. Red dashed line indicates the conventional temporal mean velocity profile, \bar{U} .

of an organised turbulent motion at this wall-normal location. It happens because the intermittent nature of the TBL is ignored in the Reynolds decomposition (i.e. the mean is calculated over regions of two different states having different velocities).

In order to overcome this problem, a new way of decomposing the total velocity is proposed, where the TBL and non-turbulent free stream are treated separately:

$$U = \tilde{U}(z, \delta_i) + u'. \quad (3.1)$$

Here $\tilde{U}(z, \delta_i)$ denotes the conditional mean velocity, which is a function of the wall-normal coordinate and the instantaneous TNTI height, δ_i ; and u' is the fluctuation about \tilde{U} . This decomposition is comparable to the triple decomposition introduced by Hussain & Reynolds (1970), although their triple decomposition isolates the periodic variation in velocity while our decomposition removes the influence of the TNTI oscillation, which is not periodic. Strictly speaking, \tilde{U} is also a function of Re_τ (just as \bar{U} is a function of Re_τ). To fully isolate the effect of the Re_τ variation, \tilde{U} needs to be computed at every streamwise grid point available (at each streamwise grid point, Re_τ is different due to the spatial growth of boundary layer). However, this requires a vast number of independent velocity vector fields to achieve a reasonable degree of convergence in \tilde{U} (having many \tilde{U} profiles at each and every streamwise grid point). Within the streamwise domain of extracted velocity fields, the variation of Re_τ and δ is not excessive (deviation of $\pm 7\%$ and $\pm 8\%$ about their nominal values for Re_τ and δ , respectively). Therefore, as a compromise to achieve a reasonable degree of convergence, the Reynolds-number variation over the 9δ domain is not accounted for in computing \tilde{U} and u' for the present study. This introduces a bias to u' such that it is shifted slightly towards the positive side around the beginning of the streamwise domain (upstream end) and towards the negative side around the end of the streamwise domain (downstream end). However, the effect of this bias on the statistics presented is marginal and not significant enough to affect the conclusions to be drawn in this paper.

Figure 2 explains how \tilde{U} is calculated. In figure 2(a), some randomly selected instantaneous total streamwise velocity profiles at streamwise locations where

$\delta_i = 0.68\delta$ are shown in grey lines. The ensemble average of all such instantaneous velocity profiles gives the conditional mean profile, \tilde{U} , for this particular δ_i (shown as the black line in figure 2a). In the wall-normal profile of \tilde{U} , the free stream and TBL are treated separately about δ_i because each \tilde{U} is computed from the instantaneous U profiles with the same TNTI location. Then, a series of \tilde{U} are computed for a range of different δ_i . Figure 2(b) shows examples of \tilde{U} at various δ_i . In cases of large TNTI oscillation, the profiles of \tilde{U} can deviate substantially from the temporal mean velocity profile (red dashed line) in the intermittent region of TBL because \bar{U} is averaged over two different states (TBL and free stream). However, the profiles of \tilde{U} and \bar{U} almost fall on top of each other in the region close to the wall. Hence, the region close to the wall will be insensitive to the decomposition method.

The fluctuating velocity component under this new decomposition can be obtained by subtracting the profiles of $\tilde{U}(z, \delta_i(x))$ from U at every streamwise location. Note that \tilde{U} varies with the streamwise position since δ_i is a function of x (and \tilde{U} is a function of δ_i and z). When the TNTI folds back onto itself (multiple TNTI locations at a given streamwise position), it is not appropriate to subtract a single continuous profile of \tilde{U} . In such cases, the region below the lowermost TNTI location and the region above the uppermost TNTI location are considered separately by subtracting the corresponding \tilde{U} for each respective region (below the lowermost TNTI location, the profile of \tilde{U} based on the lowermost TNTI location is subtracted, and above the uppermost TNTI location, the profile of \tilde{U} based on the uppermost TNTI location is subtracted). In the region between the upper- and lowermost TNTI locations (the actual region affected by the TNTI folding back), fluctuating velocity is computed about the zonal mean velocities of each respective region (Kovasznay *et al.* 1970) rather than \tilde{U} . For example, if the point of interest (residing within the TNTI folding back region) lies within the free stream, the zonal mean velocity of the free stream (the average velocity of all points that are in the free stream at a given wall-normal location) is subtracted to compute u' . Note that the actual area affected by the TNTI folding back is only approximately 1% of the total velocity fields having the streamwise and wall-normal domain of $9\delta \times 1.4\delta$.

Figure 1(c) shows the fluctuating streamwise velocity field determined using the new decomposition method. Under this new decomposition, the large-scale positive fluctuations extending into the free stream are removed (see $x/\delta \simeq 2-4$ in figure 1c). In addition, some large-scale negative fluctuations in the boundary layer (at $x/\delta \simeq 4-5$) are also removed by the new decomposition. As previously illustrated in figure 2(b), \tilde{U} for large δ_i is substantially smaller than \bar{U} in the outer region because a large proportion of free stream, which is faster than the flow in the boundary layer, is included in calculation of \bar{U} . Hence, the Reynolds decomposition (subtraction of \bar{U}) causes large-magnitude negative fluctuations in the intermittent region inside the TBL when the boundary layer is instantaneously thicker. An example illustrating the difference between the fluctuating streamwise velocity component under the two decompositions is shown in figure 1(d). It shows the streamwise velocity fluctuations under the Reynolds decomposition and our decomposition as a function of the streamwise position at $z/\delta = 0.6$. Here, the regions of the TBL that are outside of the TNTI (i.e. in the free stream) are shaded in grey and the fluctuating velocity under our decomposition (red dashed) in this region only shows the fluctuation about the free stream, so their magnitude is close to zero whereas the fluctuation is positive under the Reynolds decomposition (blue solid) in the free stream. Also, the excessive

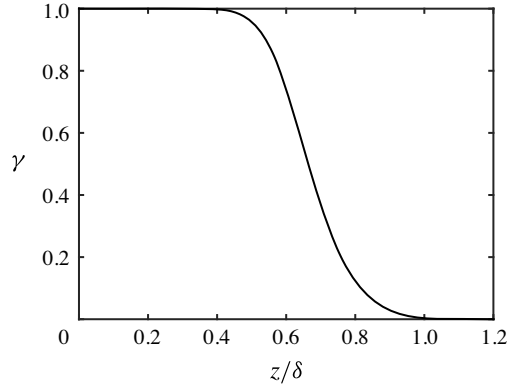


FIGURE 3. Intermittency profile of the TBL.

negative fluctuation in u , caused by an instantaneously thicker boundary layer, is removed in u' . It should be noted that the fluctuation under our decomposition is ensured to have zero temporal mean.

Overall, under the Reynolds decomposition, the oscillation of the TNTI can contaminate the fluctuating velocity components in the wake region, and it is demonstrated that the new velocity decomposition method removes this contamination. In contrast, the fluctuating velocity fields near the wall (log region and below) are not significantly altered by applying the new decomposition, suggesting that the fluctuating velocity fields near the wall are independent of the velocity decomposition method (as expected from the profiles of \tilde{U} and \bar{U} being almost the same near the wall). The other velocity components (wall-normal and spanwise) are not significantly affected by the decomposition method as compared with the streamwise velocity component, so they are not presented in this paper.

4. Effect on typical statistics

In order to quantify the degree of intermittent behaviour, the intermittency, γ , is plotted in figure 3. It is defined as the proportion of time that the flow spends in the turbulent region (Corrsin & Kistler 1955; Kovaszny *et al.* 1970); the intermittency profile of the present study agrees well with Chauhan *et al.* (2014). Up to approximately $z/\delta = 0.4$, the flow is practically non-intermittent ($\gamma = 1$). With increasing wall-normal distance from the wall, the TBL starts to exhibit the intermittent behaviour at wall-normal positions above $z/\delta = 0.4$. This suggests that the decomposition method should not affect the near-wall region since the decomposition method is only important in the intermittent region.

In order to quantitatively investigate the effect of the TNTI oscillation on the Reynolds fluctuation, pre-multiplied power spectral densities of the streamwise velocity fluctuation determined using the Reynolds decomposition ($k_x \phi_{uu}$, blue solid) and our new decomposition ($k_x \phi_{u'u'}$, red dashed) at various wall-normal positions are plotted in figure 4 as a function of energetic length scale, λ_x . An example of the streamwise velocity fluctuation signals used for computation of the spectra is shown in figure 1(d). Figure 4(a) shows the spectra at $z/\delta = 0.1$, which is within the log region. At this wall-normal position, the spectra of u and u' are very close to each other. This is consistent with the observation that the instantaneous

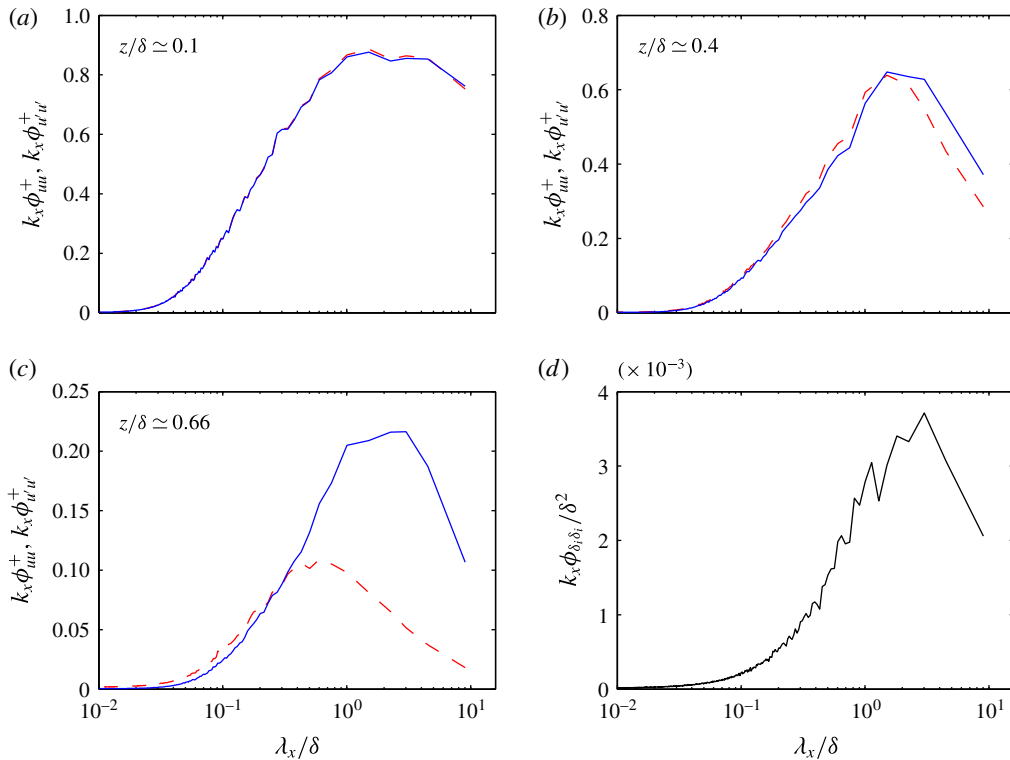


FIGURE 4. (Colour online) Pre-multiplied power spectral densities of the streamwise velocity fluctuation determined under Reynolds decomposition (blue solid) and our new decomposition (red dashed) at the wall-normal position of (a) $z = 0.1\delta$, (b) $z = 0.4\delta$ and (c) $z = 0.66\delta$. (d) Pre-multiplied power spectral density of δ_i fluctuation.

fluctuating streamwise velocity fields near the wall are not notably affected by the method of velocity decomposition. Up to approximately $z/\delta = 0.4$ (figure 4b), the spectra of u and u' do not differ from each other significantly because the flow is almost non-intermittent up to this wall-normal position, as previously mentioned. However, as we move to the wake region, where the intermittent nature of the flow is significant, the spectra of u' deviate significantly from the spectra of u . At $z/\delta = 0.66$ (where $\gamma = 0.5$), a significant amount of large-scale energy is removed from the streamwise velocity spectra when the influence of TNTI oscillation is removed by deploying our new decomposition (figure 4c). Under our new decomposition, the peak wavelength of the streamwise velocity fluctuation is shifted from $\lambda_x = (2-3)\delta$ (the typical wavelength of large-scale motions (LSMs)) to $\lambda_x \simeq 0.66\delta$, which is of the order of the wall-normal distance from the wall. In fact, the dominant wavelength of the streamwise velocity fluctuation under the Reynolds decomposition coincides with the dominant wavelength of the TNTI oscillation ($\lambda_x \simeq 3\delta$), as shown by the pre-multiplied power spectral density of δ_i in figure 4(d). In addition, the streamwise velocity fluctuation under the Reynolds decomposition is strongly anticorrelated with the fluctuation of TNTI height (the correlation coefficient between u and the fluctuating component of δ_i is approximately -0.65 at $z = 0.63\delta$), which supports the idea that in this region the streamwise velocity fluctuation under the Reynolds decomposition is strongly influenced by the TNTI oscillation. A similar

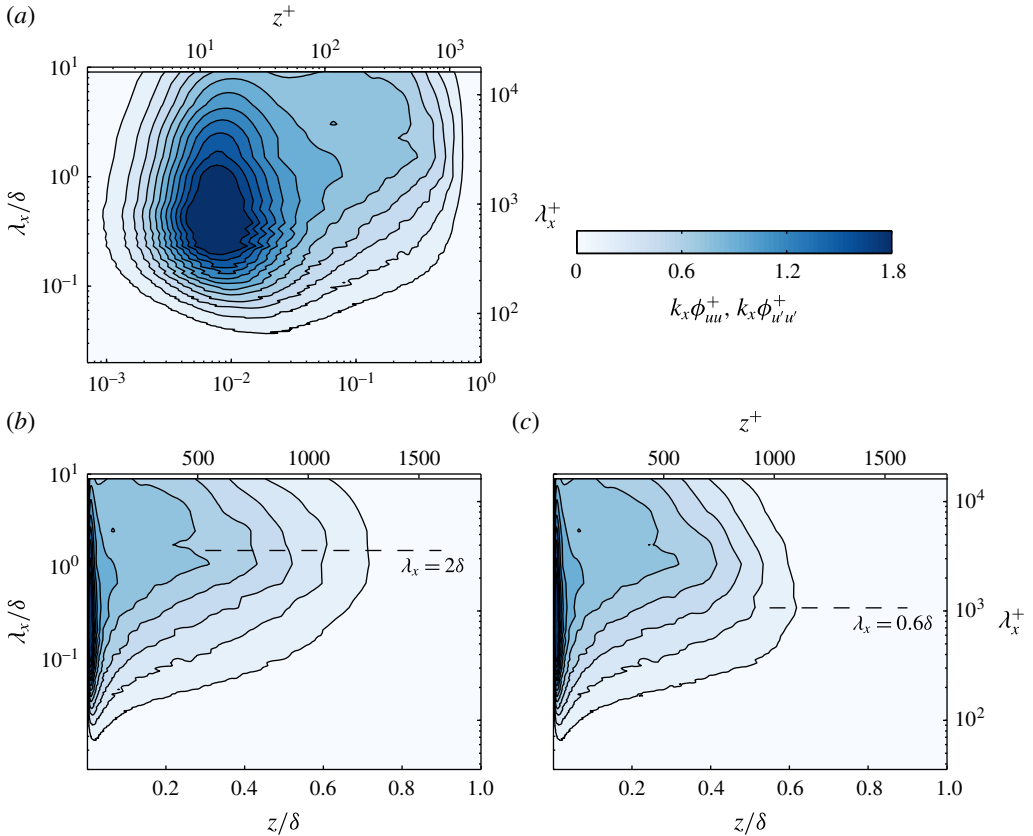


FIGURE 5. (Colour online) Pre-multiplied spectrogram of the streamwise velocity fluctuation as a function of energetic length scale and distance from the wall. The solid lines indicate the contour levels from 0.1 to 1.8 with an increment of 0.15. (a,b) Fluctuating velocity component computed using the Reynolds decomposition. (c) Fluctuating velocity component computed using the new decomposition.

remark was made by Kovaszny *et al.* (1970) from the anticorrelation between u and the intermittency function (a boxcar function whose value is 1 inside the turbulent region and 0 otherwise). Hence, in the intermittent region, the significant portion of what appears to be the large-scale energy in the spectra of streamwise velocity fluctuations under the traditional Reynolds decomposition could be just a mathematical artefact of the movement of the TNTI rather than an indication of the organised large-scale turbulent motions (with the proviso that the motion of the TNTI could, to some degree, be driven by turbulent motions). However, it needs to be made clear that the existence of the LSMs near the wall and the conclusions drawn from previous studies on them are not questioned by these results, since the effect of the velocity decomposition method on flow fields near the wall is almost negligible.

The pre-multiplied spectrograms of the streamwise velocity shown in figure 5 permit us to look at the distribution of energy over a range of energetic length scale and distance from the wall. The spectrograms of u agree well with Monty *et al.* (2009), particularly in the outer region, although the large-scale outer peak (at $z \approx 0.06\delta$ with

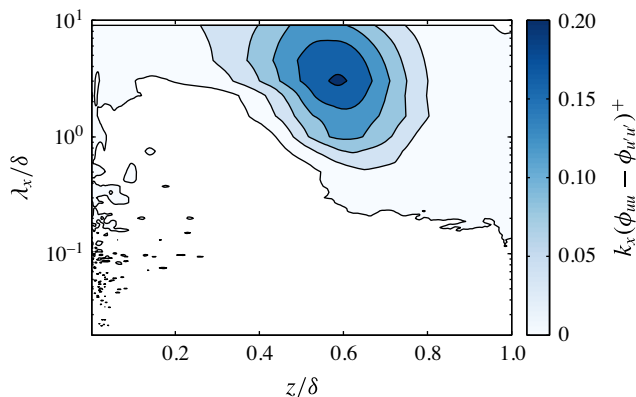


FIGURE 6. (Colour online) Difference between pre-multiplied spectrograms of streamwise velocity fluctuation under the Reynolds decomposition and the new decomposition. The solid lines indicates the contour levels from 0 to 0.2 with an increment of 0.04.

$\lambda_x \approx 6\delta$) is absent due to the low Reynolds number of this study. The common features of the spectrograms of the Reynolds fluctuations in the outer region includes the peak in the power spectra at $\lambda_x = (2-3)\delta$ (commonly referred to as LSM). The spectrograms of u' (figure 5c) reaffirm that our new decomposition removes the significant portion of energies at those very large scales and the usual LSM peak wavelength is shifted to 0.6δ throughout the intermittent region ($z > 0.4\delta$). The effect of this ‘added’ fluctuation due to the oscillation of the TNTI is better represented by looking at the difference between the power spectral densities of the streamwise velocity fluctuations under Reynolds decomposition and our decomposition (figure 6). It shows that the influence of the TNTI oscillation on the energy distribution of streamwise velocity is confined mostly within the intermittent region only at large-scale wavelengths (maximum around $z = 0.6\delta$ and $\lambda_x = 3\delta$).

The examination of the spectra of the streamwise velocity shows that the scale of turbulence is altered in the outer region when the influence of the free stream is removed by employing our decomposition. Therefore, it suggests that the large-scale coherence might not extend as far into the outer region as previously thought. In order to investigate this conjecture, the two-point correlation maps of the streamwise velocity under the Reynolds decomposition (\mathcal{R}_{uu}) and the new decomposition ($\mathcal{R}_{u'u'}$) at various reference wall-normal positions are plotted in figure 7. At the reference wall-normal position of $z = 0.1\delta$ (figure 7a,b), the two-point correlation maps under both decompositions are very similar. However, there is a hump extending into the intermittent region (the hump starts at $z \simeq 0.4\delta$ and extends up to $z \simeq 0.64\delta$ in the region of $\Delta x \simeq (1-2)\delta$) on the downstream ($\Delta x > 0$) head of the contour line at $\mathcal{R}_{uu} = 0.1$ and it is removed under our new decomposition, indicating that this hump could be due to the contamination of velocity fluctuation by TNTI oscillation. Nevertheless, the average spatial organisation of coherent velocity fluctuations in the region close to the wall is not affected by the oscillation of the TNTI, which is consistent with the instantaneous observation and spectral analysis. When \mathcal{R}_{uu} and $\mathcal{R}_{u'u'}$ about the reference position of $z = 0.4\delta$ are compared (figure 7c,d), the upstream ($\Delta x < 0$) tail of the correlation map remains almost unchanged. The inclined and wall-attached nature of the upstream tail indicates that it is associated with the flow structures that grow from the wall. In contrast, the downstream head of \mathcal{R}_{uu} ,

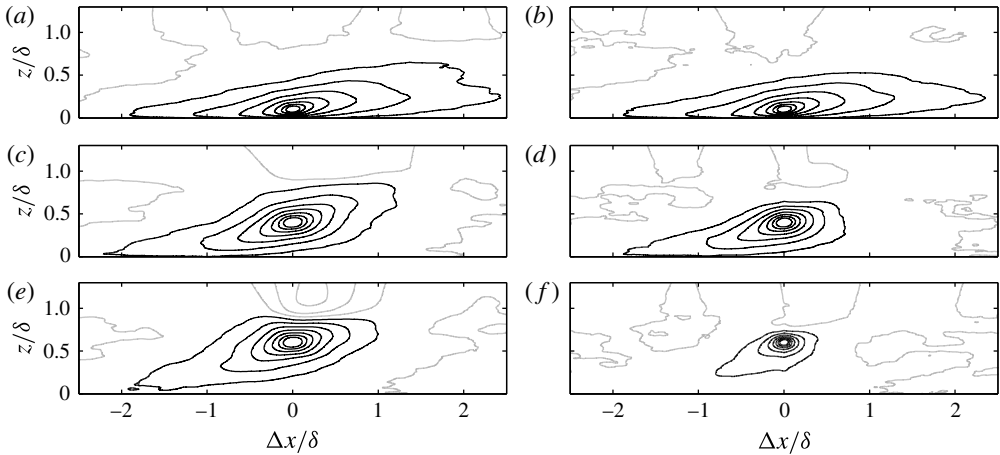


FIGURE 7. Two-point correlation map of the streamwise velocity fluctuation under the Reynolds decomposition (*a,c,e*) and the new decomposition (*b,d,f*) at the reference wall-normal position of (*a,b*) $z = 0.1\delta$, (*c,d*) $z = 0.4\delta$ and (*e,f*) $z = 0.6\delta$. The black solid lines indicate the contour levels from 0.1 to 0.7 with an increment of 0.1, and the grey solid lines indicate the contour levels of zero and below with a decrement of 0.1.

which extends into the outer region, is removed by employing our decomposition (in $\mathcal{R}_{u'u'}$). This downstream head appearing under the Reynolds decomposition (and its disappearance under the new decomposition) provides some indication that there is a connection between the motion of the TNTI and the velocity fluctuation at the reference point of 0.4δ (the motion of the TNTI appears as large-scale velocity fluctuations in the outer region). Albeit weak, this relationship even extends close to the wall ($z = 0.1\delta$) as observed by the existence of the ‘hump’ described earlier (figure 7*a*). The difference between \mathcal{R}_{uu} and $\mathcal{R}_{u'u'}$ becomes more dramatic when the reference wall-normal position is in the middle of the intermittent region. Figure 7(*e,f*) shows \mathcal{R}_{uu} and $\mathcal{R}_{u'u'}$ at the reference wall-normal position of $z = 0.6\delta$. Here, the overall shape of \mathcal{R}_{uu} and $\mathcal{R}_{u'u'}$ is similar but $\mathcal{R}_{u'u'}$ extends much less spatially. The inclined upstream tail of $\mathcal{R}_{u'u'}$ indicates that inclined flow structures do extend up to the intermittent region, but the average extents of these structures are exaggerated under the Reynolds decomposition. In addition, the contour line of $\mathcal{R}_{uu} = 0.1$ has a flat top and this is a likely consequence of the regions of positive streamwise velocity fluctuation existing into the free stream (figure 1*b*), which also have a flat top as a result of subtracting the gradually varying \bar{U} profile from the constant free-stream velocity.

5. Conclusions

In the structural analysis of TBLs, the perils of applying the Reynolds decomposition in the intermittent region of a TBL to determine the fluctuating component of the streamwise velocity are demonstrated. This is caused by ignoring the intermittent behaviour of the flow and overlooking the effect it has on the fluctuating velocity components under the Reynolds decomposition. Instantaneous observations are made that the oscillation of the TNTI contaminates the streamwise velocity fluctuations around the intermittent region. This influence is removed by applying a new method of decomposing the total velocity where the turbulent region and non-turbulent free

stream are considered separately. However, it should be noted that it is not within the scope of this paper to comment on the suitability of the Reynolds decomposition for other purposes such as turbulence modelling.

The comparison of pre-multiplied power spectral densities of the streamwise velocity fluctuations under both decompositions in the outer region of a TBL reveals that the dominant wavelength, $(2-3)\delta$, of the streamwise fluctuating velocity under the Reynolds decomposition is dictated by the dominant wavelength of the TNTI oscillation. The dominant wavelength of the streamwise fluctuating velocity under our new decomposition is approximately 0.6δ . In addition, a significant portion of what appears to be the large-scale energy under the Reynolds decomposition is removed when our new decomposition is employed. The general shape and scale of the two-point correlation map of the streamwise velocity fluctuation is similar under both decompositions below the intermittent region. However, in the intermittent region, the two-point correlation map under the Reynolds decomposition is contaminated by the TNTI oscillation, resulting in the overestimated spatial extent of organised turbulent motions compared to when our new decomposition is used (i.e. when the influence of the TNTI oscillation on the velocity fluctuation is removed).

Acknowledgements

The authors wish to acknowledge the financial support of the Australian Research Council. Y.S.K. was partially supported by the Defence Science and Technology Organisation. The authors are grateful to Dr J. A. Sillero and Professors J. Jiménez and R. D. Moser for making the DNS dataset publicly available.

REFERENCES

- ANTONIA, R. A. 1972 Conditionally sampled measurements near the outer edge of a turbulent boundary layer. *J. Fluid Mech.* **56**, 1–18.
- ANTONIA, R. A., PRABHU, A. & STEPHENSON, S. E. 1975 Conditionally sampled measurements in a heater turbulent jet. *J. Fluid Mech.* **72**, 455–480.
- CHAUHAN, K., PHILIP, J., DE SILVA, C., HUTCHINS, N. & MARUSIC, I. 2014 The turbulent/non-turbulent interface and entrainment in a boundary layer. *J. Fluid Mech.* **742**, 119–151.
- CHAUHAN, K. A., MONKEWITZ, P. A. & NAGIB, H. M. 2009 Criteria for assessing experiments in zero pressure gradient boundary layers. *Fluid Dyn. Res.* **41**, 021404.
- CORRSIN, S. 1943 Investigation of flow in an axially symmetrical heated jet of air. *NACA WR W-94*.
- CORRSIN, S. & KISTLER, A. L. 1955 Free-stream boundaries of turbulent flows. *NACA Rep.* **1244**, 1033–1064.
- FABRIS, G. 1979 Conditional sampling study of the turbulent wake of a cylinder. Part 1. *J. Fluid Mech.* **73**, 465–495.
- GUTMARK, E. & WYGNANSKI, I. 1976 The planar turbulent jet. *J. Fluid Mech.* **73**, 465–495.
- HEDLEY, T. B. & KEFFER, J. F. 1974 Some turbulent/non-turbulent properties of the outer intermittent region of a boundary layer. *J. Fluid Mech.* **64**, 645–678.
- HUSSAIN, A. K. M. F. & REYNOLDS, W. C. 1970 The mechanics of an organized wave in turbulent shear flow. *J. Fluid Mech.* **41**, 241–258.
- HUTCHINS, N. & MARUSIC, I. 2007 Evidence of very long meandering features in the logarithmic region of turbulent boundary layers. *J. Fluid Mech.* **579**, 1–28.
- KOVASZNYI, L. S. G., KIBENS, V. & BLACKWELDER, R. F. 1970 Large-scale motion in the intermittent region of a turbulent boundary layer. *J. Fluid Mech.* **41**, 283–325.
- LYN, D. A. & RODI, W. 1994 The flapping shear layer formed by flow separation from the forward corner of a square cylinder. *J. Fluid Mech.* **267**, 353–376.

- MONTY, J. P., HUTCHINS, N., NG, H. C. H., MARUSIC, I. & CHONG, M. S. 2009 A comparison of turbulent pipe, channel and boundary layer flows. *J. Fluid Mech.* **632**, 431–442.
- REYNOLDS, O. 1895 On the dynamical theory of incompressible viscous fluids and the determination of the criterion. *Phil. Trans. R. Soc. Lond.* **186**, 123–164.
- SILLERO, J. A., JIMÉNEZ, J. & MOSER, R. D. 2013 One-point statistics for turbulent wall-bounded flows at Reynolds numbers up to $\delta^+ \approx 2000$. *Phys. Fluids* **25**, 105102.
- SILLERO, J. A., JIMÉNEZ, J. & MOSER, R. D. 2014 Two-point statistics for turbulent boundary layers and channels at Reynolds numbers up to $\delta^+ \approx 2000$. *Phys. Fluids* **26**, 105109.
- TOMKINS, C. D. & ADRIAN, R. J. 2003 Spanwise structure and scale growth in turbulent boundary layers. *J. Fluid Mech.* **490**, 37–74.
- WYGNANSKI, I. & FIEDLER, H. E. 1970 The two-dimensional mixing region. *J. Fluid Mech.* **41**, 327–361.